

Comparison between hybrid CBCT and CBCT in detection of vertical root fracture



A Thesis Submitted in Partial Fulfillment of the Requirements
for the Degree of Master of Science in Oral and Maxillofacial Radiology

Department of Radiology

FACULTY OF DENTISTRY

Chulalongkorn University

Academic Year 2019

Copyright of Chulalongkorn University

การเปรียบเทียบระหว่างเครื่องซีพีซีทีแบบผสมและซีพีซีทีในการตรวจหารากฟันแตกในแนวดิ่ง



วิทยานิพนธ์นี้เป็นส่วนหนึ่งของการศึกษาตามหลักสูตรปริญญาวิทยาศาสตรมหาบัณฑิต

สาขาวิชารังสีวิทยาช่องปากและแม็กซิลโลเฟเชียล ภาควิชารังสีวิทยา

คณะทันตแพทยศาสตร์ จุฬาลงกรณ์มหาวิทยาลัย

ปีการศึกษา 2562

ลิขสิทธิ์ของจุฬาลงกรณ์มหาวิทยาลัย

Thesis Title Comparison between hybrid CBCT and CBCT in detection
of vertical root fracture
By Mrs. Nantida Rueangweerayut
Field of Study Oral and Maxillofacial Radiology
Thesis Advisor VANNAPORN CHUENCHOMPOONUT, Ph.D

Accepted by the FACULTY OF DENTISTRY, Chulalongkorn University in Partial
Fulfillment of the Requirement for the Master of Science

..... Dean of the FACULTY OF
DENTISTRY
(Assistant Professor SUCHIT POOLTHONG, Ph.D.)

THESIS COMMITTEE

..... Chairman
(Clinical Professor WICHITSAK CHOLITGUL)

..... Thesis Advisor
(VANNAPORN CHUENCHOMPOONUT, Ph.D)

..... Examiner
(Assistant Professor CHOOTIMA RATISOONTORN, Ph.D.)

นันทิดา เรื่องวีรยุทธ : การเปรียบเทียบระหว่างเครื่องซีบีซีทีแบบผสมและซีบีซีทีในการตรวจหารากฟันแตกในแนวดิ่ง. (Comparison between hybrid CBCT and CBCT in detection of vertical root fracture) อ.ที่ปรึกษาหลัก : อ.ทญ.ดร.วรรณภรณ์ ชื่นชมพูนุท

ในปัจจุบันการถ่ายภาพรังสีซีบีซีทีที่มีบทบาทสำคัญในการตรวจหาการเกิดรากฟันแตกในแนวดิ่งเป็นอย่างมาก อย่างไรก็ตามเครื่องซีบีซีทีที่มีราคาค่อนข้างแพงเมื่อเทียบกับเครื่องถ่ายภาพรังสีในช่องปากและนอกช่องปากแบบที่ใช้กันอยู่ทั่วไป ดังนั้นเพื่อเป็นการตอบสนองความต้องการของผู้ใช้งานในปัจจุบันจึงได้มีการพัฒนาเครื่องซีบีซีทีที่เรียกว่า เครื่องซีบีซีทีแบบผสม เพื่อให้สามารถตอบสนองความต้องการของผู้ใช้งานที่หลากหลายมากขึ้น รวมถึงเพื่อลดราคาและขนาดของเครื่องซีบีซีทีลงให้มีความเหมาะสมสำหรับการใช้งานในคลินิกทันตกรรมทั่วไป การศึกษานี้มีวัตถุประสงค์เพื่อเปรียบเทียบความแตกต่างในการตรวจหารากฟันแตกในแนวดิ่งระหว่างเครื่องซีบีซีทีแบบผสมและเครื่องซีบีซีที โดยการศึกษานี้ใช้ฟันกรามน้อยล่างจำนวน 40 ซี่ที่ผ่านการเตรียมคลองรากฟันแล้ว และจะถูกนำมาใส่ลงในขากรรไกรล่างของมนุษย์บริเวณฟันกรามน้อยล่างซี่ที่ 2 จากนั้นทำไปถ่ายภาพรังสีด้วยเครื่องซีบีซีทีและเครื่องซีบีซีทีแบบผสม ด้วยมาตรการที่หลากหลาย จากนั้นผู้วิจัยจำนวน 3 ท่านจะทำการตรวจหารากฟันแตกในแนวดิ่งจากภาพรังสีทั้งหมด ผลการศึกษาพบว่า ทั้งเครื่องซีบีซีทีและเครื่องซีบีซีทีแบบผสม สามารถตรวจหารากฟันแตกในแนวดิ่งได้ไม่แตกต่างกัน โดยพบว่าเครื่องซีบีซีทีสามารถใช้ตรวจหารากฟันแตกในแนวดิ่งได้ดีกว่าเครื่องซีบีซีทีแบบผสมอย่างไม่มีนัยยะสำคัญ นอกจากนี้ยังพบว่า ยิ่งเล็กลงให้ขอบเขตการมองเห็น (Field of view - FOV) ที่มีขนาดเล็ก ยิ่งสามารถตรวจพบรากฟันแตกในแนวดิ่งได้ดีมากขึ้น และนอกจากนี้ยังพบว่าการที่มีวัสดุอุดคลองรากฟันอยู่จะทำให้ความสามารถในการตรวจหารากฟันแตกในแนวดิ่งของทั้งเครื่องซีบีซีทีและซีบีซีทีแบบผสมลดลง อย่างไรก็ตามในอนาคตยังคงต้องมีการทำการศึกษาเพิ่มเติมต่อไป

สาขาวิชา	รังสีวิทยาช่องปากและแม็กซิลโลเฟเชียล	ลายมือชื่อนิสิต
ปี	2562	ลายมือชื่อ อ.ที่ปรึกษาหลัก
การศึกษา		

6075819832 : MAJOR ORAL AND MAXILLOFACIAL RADIOLOGY

KEYWORD: CBCT, Hybrid CBCT, Vertical root fracture

Nantida Rueangweerayut : Comparison between hybrid CBCT and CBCT in detection of vertical root fracture. Advisor: VANNAPORN CHUENCHOMPOONUT, Ph.D

Cone beam computerized tomography (CBCT) has been widely used in many fields of dentistry, especially to investigate the vertical root fracture (VRF). CBCT systems were consisted of various field of view (FOV). As for high cost and large machine size, newly designed of CBCT systems started to develop by combining digital panoramic radiographs with a relatively small-to-medium FOV CBCT system. These new model of CBCT systems was called hybrid CBCT. The aims of this study is to compare the difference in detection of VRF by a hybrid CBCT and a CBCT. For this, forty permanent mandibular premolar teeth were endodontically prepared and individually inserted dry human mandible. All teeth were scanned with two CBCT systems by using various scanning protocols. Three observers were randomly evaluated all radiographic images. As a result, CBCT and hybrid CBCT have similar abilities in detecting VRF, however, CBCT system show a slightly higher performance. Moreover, with smaller FOV and voxel size, better VRF detection can be achieved. Furthermore, presentation of root canal filling material can reduce diagnostic ability of the VRF for overall CBCT systems. In conclusion, detection of VRF with hybrid CBCT is not significantly different from that in CBCT system. However, further researches are required.

Field of Study:	Oral and Maxillofacial Radiology	Student's Signature
Academic Year:	2019	Advisor's Signature

ACKNOWLEDGEMENTS

I would like to express my appreciation to all those who have helped to make this thesis success. Gratefully thank you for my advisor Dr. Vannaporn Chuenchompoonut and Dr. Onanong Silkosessak for a very helpful guidance in every steps of this research project. A special acknowledgment would also be showed to Assist. Prof. Dr. Soranum Chantarangsu for her kindness in statistic consultation. Sincere appreciation to all members of my committee and examiner: Clinical Professor Wichitsak Cholitkul and Assist. Prof. Dr. Chootima Ratisoontorn.

Tribute must be paid to all teachers and staffs in department of Oral and Maxillofacial Radiology, Faculty of Dentistry, Chulalongkorn University for every support and encouragement.

Nantida Rueangweerayut

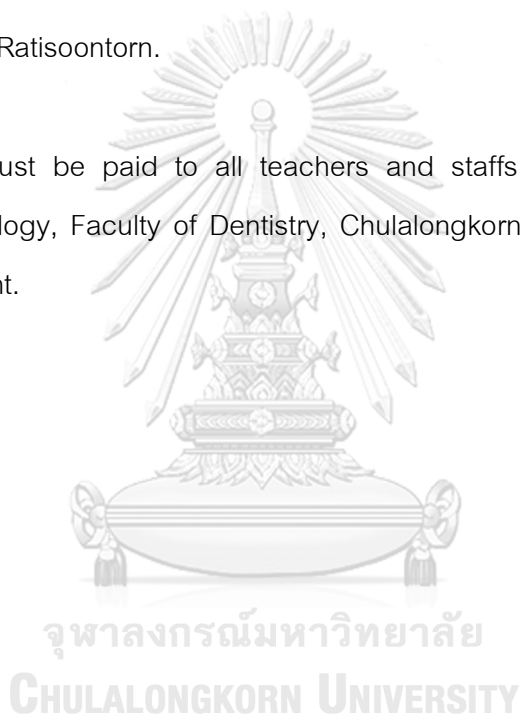


TABLE OF CONTENTS

	Page
.....	iii
ABSTRACT (THAI).....	iii
.....	iv
ABSTRACT (ENGLISH)	iv
ACKNOWLEDGEMENTS.....	v
TABLE OF CONTENTS.....	vi
LIST OF TABLES.....	1
LIST OF FIGURES	2
CHAPTER I: INTRODUCTION	3
Background and Rationale	3
Objectives	6
Scope of study	6
Expected benefits	7
CHAPTER II: LITERATURE REVIEW.....	8
Vertical root fracture.....	8
CBCT modalities	11
Metal artifact: Definition and cause	13
Soft tissue simulation	15
Conceptual Framework.....	16
Research hypothesis	16
CHAPTER III: MATERIAL AND METHOD.....	17

Sample size	17
Inclusion criteria	17
Exclusion criteria	17
Sample size calculation.....	18
Preoperative tooth preparation	18
Tooth preparation.....	18
Radiographic phantom preparation	19
Image scanning	20
Image analysis	22
Statistical analysis	25
CHAPTER IV: RESULT & DISCUSSION	26
Result.....	26
Fracture analysis	26
Interobserver agreement and intraobserver agreement	27
Detection of the vertical root fracture.....	28
Discussion.....	32
Conclusion	37
REFERENCES.....	38
VITA	48

LIST OF TABLES

	Page
Table 1 Interobserver agreement in the detection of vertical root fracture.....	27
Table 2 Diagnostic performance of each CBCT modalities	28
Table 3 Diagnostic performance of each scanning protocols	29
Table 4 Area under ROC curved showing diagnostic performance of hybrid CBCT and CBCT using 2 different FOVs	29
Table 5 Sensitivity and specificity in VRF detection with 4x4 and 8x8 cm FOV from hybrid CBCT and CBCT using 2 difference FOVs.....	30
Table 6 Area under ROC curved showing diagnostic performance of hybrid CBCT and CBCT with and without Gutta percha cone	30
Table 7 Sensitivity and specificity in VRF detection with 4x4 and 8x8 cm FOV from hybrid CBCT and CBCT with and without Gutta percha cone	31
Table 8 CTDIvol of each CBCT in difference FOVs as shown in operation guideline	33

LIST OF FIGURES

	Page
Figure 1 Tooth with incomplete root fracture (B.) and complete root fracture (C.).....	8
Figure 2 Two pieces of 1.0 mm thick copper filters were attached to the CBCT machine (Veraviewepocs 3D R100 and 3D Accuitomo 170)	19
Figure 3 Sample fixed in 2 x 2.5 cm (diameter x height) PVC tube with resin acrylic	21
Figure 4 VRF creation by using a universal testing machine (hounsfield H10KM, test equipment Ltd, Redhill, United Kingdom)	22
Figure 5 An example of an axial cross-section showing a vertical root fracture of hybrid CBCT (Veraviewepocs 3D R100) and CBCT (3D Accuitomo 170) using 4x4 and 8x8 cm FOV	23
Figure 6 Location of fracture line recorded for score 4 and 5	24
Figure 7 The micro CT images of 10% randomly selected teeth with VRF	26

CHAPTER I: INTRODUCTION

Background and Rationale

Vertical root fractures are one of the most difficult clinical problems to diagnose and treat. They have also been reported as the third most common cause of tooth loss after dental caries and periodontal disease (1). Most of vertical root fractures occur in endodontically treated teeth and have the symptoms similar to those of chronic apical periodontitis or chronic periodontitis (2). Due to these unspecific sign and symptoms, the diagnosis of vertical root fractures are difficult and often requires prediction rather than definitive identification (3). Conventional and digital two-dimensional intraoral radiography has been most common modalities in detecting vertical root fractures in routine clinical practice (4). However, there are also a limitation because vertical root fractures can only be seen on the periapical radiographs when the central x-ray beam is parallel to the fracture line. Presentation of the radiolucent fracture line give the radiographic diagnosis of the vertical root fracture but absence of these line can occur due to superimposition of adjacent structures and give the false negative diagnosis instead (5).

Since cone beam computed tomography (CBCT) was introduced to dentistry, this technology offered three-dimensional (3D) visualization, with high resolution accurate information of hard tissues whereas a relatively low radiation dose. These make

CBCT been recognized as an important diagnostic tool as they have great potential for diagnostics, treatment planning and follow up of the patients in many fields of dentistry in past two decades including implantology, surgery, orthodontics and endodontic. Thus CBCT has become a valuable imaging modality in dentistry and is increasingly use (6). As for the vertical root fracture, limited field of view CBCT imaging has been organized by the American Association of Endodontics as the imaging modality of choice for the diagnosis and management of the root fractures (7).

The size of the FOV significantly affected the evolution of the CBCT scanner (8). Initially, CBCT units were produced with limited ability to adjust the FOV and were either full maxillofacial units or small FOV. As CBCT equipment market has matured, more CBCT units with a selection of various FOVs were also available (9). The CBCT unit can be grouped into 3 categories based on maximum vertical FOV as follow (10);

A small or limited FOV cover approximately 5 cm diameter or less. This small FOV CBCT have the capability of high spatial resolution and ability to visualize changes to the periodontal ligament spaces or lamina dura, root fractures, periapical lesions, relationship of an impacted tooth with the surrounding anatomical structures, and root canal morphology. Thus, this type of CBCT scanner is normally used for endodontic purposes.

A medium FOV referred to the scans that are approximately 6 - 11 cm in height and cover one arch or both dental arches. Normally, this type of scan is used for evaluation of the extent of a lesion, status of the temporomandibular joints and implant planning cases.

A large FOV is recommended for specific cases with skeletal anomaly/asymmetry and where orthodontic/orthognathic surgery is planned. The scanned area may range from 11 to 24 cm in height and covers most of the craniofacial skeleton.

Nowadays, the evolutionary of CBCT has developed a new branch which is the “hybrid CBCT” (11). This new CBCT system combines with digital conventional 2-dimensional (2D) dental imaging feature such as panoramic radiograph or cephalometric radiograph in same unit with a relatively small to medium FOV CBCT system. As a result, these kinds of architecture are space saving and lower cost investment compare to another one (12, 13).

However, disadvantage of CBCT images are the appearance of the artifacts which are often cause of decreasing in image quality and lead to the misdiagnosis. Artifact is any distortion or error in the image that is unrelated to the subject (14). Many parameters such as field of view, X-ray beam quality and quantity, pixel size and arc of rotation may affect the CBCT image diagnostic quality.

In detection of VRF, there are many research works have studies about the accuracy among various modalities, such as conventional and digital periapical radiograph (PR) and comparing among each CBCT modalities concerning exposure parameters, voxel size and the influence of tooth orientation in detection of the vertical root fracture. However, to our knowledge, there are no previous study comparing between the different types of CBCT before.

Objectives

The aim of this study is to compare the difference in detection of the vertical root fracture by a hybrid CBCT and a CBCT.

Scope of study

This study is scoped in experimental laboratory study. Human premolar will be scanned using CBCT and hybrid CBCT both before and after vertical root fracture is created. Image analysis will be performed by using i-Dixel software provided by each CBCT machine. The receiver operating characteristic (ROC) curve will be calculated to assess the relationship between the sensitivity and specificity of both CBCT machine in the diagnosis of root fracture.

Expected benefits

This study will provide the preliminary data for the consideration in selection of CBCT modalities when vertical root fracture is suspected. Whether the hybrid CBCT can be used without any difference from CBCT in detection of vertical root or not, can be answer based on this study.



CHAPTER II: LITERATURE REVIEW

Vertical root fracture

According to the American Association of Endodontics (AAE), vertical root fracture (VRF) is defined as a longitudinally oriented fracture initiated from the root at any level and may extend coronally toward the cervical periodontal attachment (15). VRF will extend laterally from the root canal wall to the root surface and can be result in 2 type of VRF based on the visibility of the separated fragments as incomplete and complete root fracture. An absence of separation referred to incomplete VRF while a complete fracture have visible separation (16, 17).

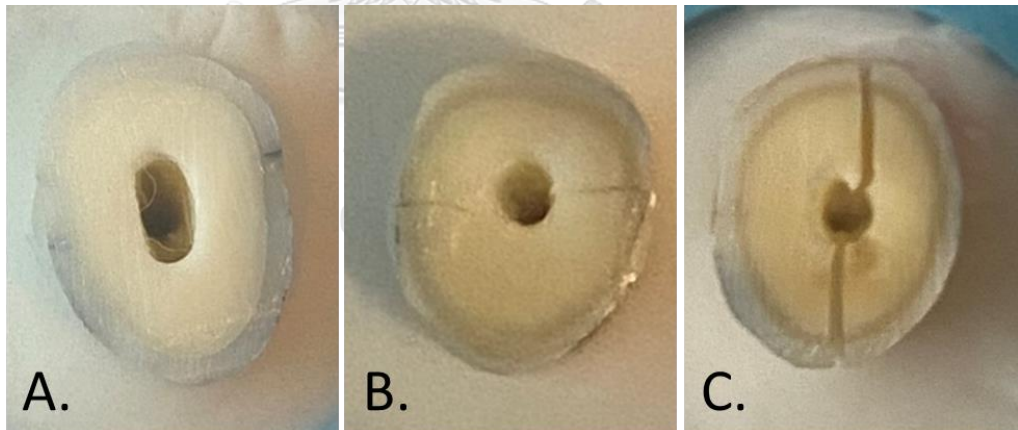


Figure 1 Tooth with incomplete root fracture (B.) and complete root fracture (C.)

VRFs have been reported to occur in both endodontically and non-endodontically treated teeth. But the majority occur in endodontically treated teeth, with

a prevalence of 11% -20% were reported (18). Yoshino K et al. (19) study showed that the tooth types with the highest percentage of extractions due to VRF were lower first molar and lower second premolar. Thus, in this study, premolar teeth will be selected as the sample group.

Major factors that induce the VRFs include excessive root canal preparation, extreme lateral and vertical compaction forces during the process of root canal filling, moisture loss in pulpless teeth, overpreparation of post space, excessive pressure during post placement, and compromised tooth integrity as a result of large carious lesions or trauma (20). In non-endodontically treated teeth, excessive occlusal forces following biting on hard objects or malocclusions are the main cause of VRF (21). Extension of the VRF in to the periodontal ligament, and soft tissue result resorption of surrounding bone which enlarge over time negatively affecting the possibility of further treatment in the affected area (22). Rapid diagnosis of a VRF is required to prevent additional bone loss that will further impact the further treatment (23).

Due to unspecific clinical feature which indicates the presentation of root fracture and the delayed showing of signs and symptoms are often make the diagnosis of the VRF become difficult (24). As the exacerbation of root fracture develops, discomfort may occur follow along with mild pain at area adjacent to fractured tooth, dull pain on mastication, gingival swelling, a fistula or sinus tract, sensitivity to percussion and palpation, and deep localized periodontal probing defects (25).

The radiographic sign of VRF can be varies from case to case depending on the angle of the X-ray beam the time after fracture and the degree of VRF separation (24). A radiolucent line between the fragments along with a discontinuity of the periodontal ligament shadow can represent the VRF in radiographic images (26). Another common radiographic sign of VRF is the “halo” appearance, which can be described as either “combined periapical and perilateral radiolucency along the side of the root, lateral periodontal radiolucency along the side of the root, or angular radiolucency from the crestal bone terminating along the root side” (27). However the two-dimensional nature of conventional intraoral radiographs, with the superimposition of other structures, limits its sensitivity for VRF detection (28). CBCT allow the dental practitioners to visualize the teeth three-dimensionally and higher resolution which can overcome the inherent disadvantages of these anatomical superimposition, Thus, CBCT has been used for proper diagnosis of the VRF (26). Nevertheless, the most accurate method to ascertain the diagnosis of VRF, now a day, is a surgical revision or visual inspection of the extracted root (29). Surgical exploratory flap surgery combining with magnification device, staining or transillumination can be used as an option for the final diagnosis and treatment planning when clinical and radiographic examinations offer only limited information (18, 24, 30). A study from Ghorbanzadeh et al.(31) also reported that using transillumination integrate with methylene blue staining has highest sensitivity in

detection of apical root end crack followed by using transillumination and methylene blue staining respectively.

CBCT modalities

It is reported that IIT/CCD detectors are inferior to FPD in terms of reduced dynamic range, contrast and spatial resolution, increased pixel noise, and image artifacts (32).

Technical factors such as kVp and mA also have an effect on the image quality of CBCT. Higher X-ray tube potential (kVp) will increase penetration of the X-ray beam through metal and theoretically can reduce the metal artifact. But increasing kVp can result in lower contrast in the image and also have the effect of increasing radiation dose to the patient. Higher X-ray tube current (mA) can result in more photons detected which reduce the noise in the image and, therefore, decrease the metallic artifacts (33).

Field of view (FOV) referred to the size of the scanned object volume and also be another important parameter that may influence dental diagnosis (8). Selection of appropriate FOV is important for gaining most proper image based on the disease presentation and the designated imaging region for each patient (2). Some studies have described that a small FOV result in higher accuracy for the diagnosis of root fracture (5). Smaller FOV can avoid artifact interference and also patient radiation exposure. To

reduce the image processing time, a corresponding voxel is usually needed with the FOV.

Voxel size is the smallest 3D element of the volume. A smaller voxel was reported to be better for detection of VRF (2). There is also a study reported that 0.2-mm voxel size is the best choice for diagnostic of VRF, considering the ALARA principle (34).

As mention before, two type of CBCT modalities have been categorized which are hybrid CBCT and a CBCT. Among these 2 types, a hybrid CBCT machine tends to have lower dose and shorter scan time due to a small size of FOV. Anyhow, some hybrid CBCT modality also have a limit in degree of rotation and vertical angulation of cone beam which may impact on image quality and artifacts (13).

There is a study present that limited volume CBCT scans with 360° of rotation have higher radiation dose associated with the higher degree of rotation and also have no better in detecting the external root resorption than same CBCT scans with 180° of rotation (35). However, another study reported that there are fewer artifacts and higher image quality when using a device with 360° of rotation when compared with 270° of rotation in evaluated image quality of CBCT images adjacent to titanium dental implants (36). Eventually, there also a study demonstrate that a hybrid CBCT machine could reach as equivalent performances as a CBCT one (12).

Metal artifact: Definition and cause

Metal artifact are known as common problem in CBCT image because these streak artifacts not only appear because of the presence of metallic prosthetic but are also caused by presented of other material used in dentistry such as dental filling material, root canal filling material and orthodontic appliances (37).

The starbursts or streaks artifact which are typically seen in radiographic image where metallic object is presented in the area of interest which occur due to the density of the metal is beyond the normal range that can be handled by the computer and resulting in incomplete attenuation profiles and refer as metal artifact (38).

Metal artifacts apparently decrease the quality of CBCT images by increasing background noise with a simultaneous decrease the image contrast.

Beam hardening is a phenomenon when the X-ray beam pass through an object, the low-energy photons are absorbed more than the high-energy photons which increase means energy and result in two types of artifact; cupping artifacts and the dark bands or streaks (39). Cupping artifact occur when a uniform cylindrical object is imaged and the X-rays beam passing through the middle portion of are hardened more than those passing though the edges and presented as distortion of the object (40). Nevertheless, this cupping effect was more prominent in large-FOV image acquisitions, and did not cause a distortion in the metal image at its edge, but did cause a distortion in its inner portion. In CBCT image, from small FOV scanners, the cupping artifact was

indistinguishable from other artifacts in the images (41). Due to only the higher energetic rays penetrate the high density object, the sensor will records too much energy and the back projection process of these 'overestimated' intensities will produce dark streaks anywhere (6). The portion of the beam that passes through one of the objects at certain tube positions is hardened less than when it passes through both objects at other tube positions can also create the streak or dark band between two dense structure and darken of the regions adjacent to, or surrounded by, structures (42).

Scatter is produced by off-axis low-energy radiation that is generated in the patient during image acquisition. It corresponds to those photons that are diffracted from their original path after interaction with matter and reach the detector not attributable to the incident primary beam. Scatter can be presents as the radiopaque lines and patterns of metallic density that "scatter" on image reconstructions which are very similar to those streak pattern caused by beam hardening phenomenon (8, 43, 44).

The manner of metal artifact presented in the image is varies depends on the severity of these effects according to many other factors which effect the energy of the incident photons and the detection of the transmitted X-ray beam by the image detector in the scanner and the way the reconstruction algorithm process. (37, 42)

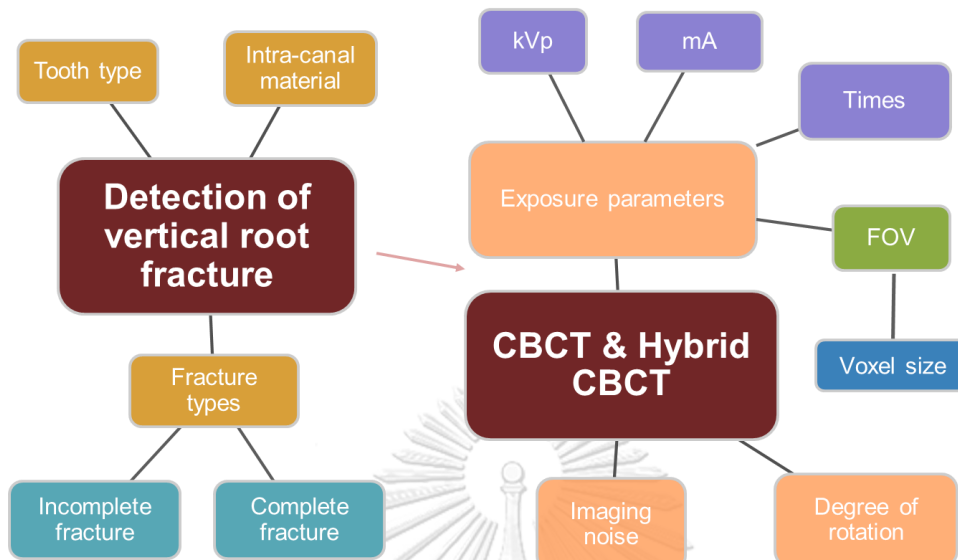
Soft tissue simulation

Human jaws are heterogeneous structures composed of diverse types of hard and soft tissues. Thus, trying to simulate soft tissue in order to imitate the beam attenuation effect of soft tissue is essential so that the images will be as similar as possible to patients' images makes the methodological approach more realistic. There are many materials have been used to simulate the soft tissue model for human dry skull such as acrylic plate, dental wax, water and copper filter.

There is a study that mimic the x-ray beam attenuation of soft tissue by placing a 1 cm thick acrylic plate between the x-ray source and the specimen. This acrylic plate will reproduce the absorption and scatter created during clinical CBCT imaging as the X-ray beam encounters the cervical spine and other areas of the mandible (35). Another study whose coated the skull with a layer of 5 mm thick dental wax and then immersed in a Styrofoam box filled with water or a total thickness of 10 mm cover the bone surface to provide images similar to clinical situations by simulating the soft tissue (41, 45). There also a study that use A 1.7 mm thick copper filter to mimic soft tissue attenuation during image acquisition to prevent any overexposures (46).

In this study, two pieces of 1.0 mm thick copper filters will be used to simulate the soft tissue model.

Conceptual Framework



Research hypothesis

Detection of vertical root fracture with hybrid CBCT is not different from that in CBCT.

CHAPTER III: MATERIAL AND METHOD

This study was conducted with approval from the Human research ethics committee of faculty of Dentistry, Chulalongkorn University (HREC-DCU 2019-030).

Sample size

Extracted human permanent premolar teeth will be collected according to inclusion and exclusion criteria as shown below.

Inclusion criteria

1. Straight and single canal
2. No vertical root fracture detected by 1% methylene blue

Exclusion criteria

1. Previously root canal treated
2. Root caries exposed pulp
3. Root resorption
4. Pulp calcification or canal obliteration
5. Incomplete root formation (open apex)

All teeth will be assigned into 4 groups: 2 experimental groups (VRF + filling, no-VRF + filling) and 2 control groups (positive control: VRF + no-filling, negative control: no-VRF + no-filling)

Sample size calculation

Data from the research work of Elsaltani et al. (47) were used to calculate sample size using below formula

$$n = \frac{\left(z_{1-\alpha} + z_{1-\frac{\beta}{2}}\right)^2}{(\delta - |\epsilon|)^2} \left[\frac{p_1(1-p_1)}{k} + p_2(1-p_2) \right]$$

When $\epsilon = p_1 - p_2$

$$p_1 = 0.703 \quad p_2 = 0.816 \quad \delta = 0.4 \quad \alpha = 0.05 \quad \beta = 0.2$$

Thus, the sample size for each group is 36 teeth which will be round up to 40 teeth.

Preoperative tooth preparation

All extracted teeth were stored in 10% formalin solution soon after tooth extraction. Gracy curette hand scaler was used to clean tooth surface by removing soft tissue debris and dental calculus, then the periapical radiographs were performed to rule out any tooth with exclusion criteria. A 1% methylene blue combining with trans illumination were acquired for the absence of vertical root fracture and then will be kept moist in 10% formalin until vertical root fractures were induced.

Tooth preparation

All teeth were decoronated with high speed cylinder diamond bur at 2 mm above cemento-enamel junction level to eliminate a bias of enamel fractures. The root

canals were prepared with ProTaper NEXT rotary system (Dentsply Maillefer, Tulsa, OK) until file size X3 (30/.07) and irrigated with distilled water.

Radiographic phantom preparation

A dry human mandible was used as a radiographic phantom for this experiment. The second premolar socket was selected and carefully prepared with a cylindrical diamond bur to obtain a passive fit of the roots, then each sample will be placed in this socket individually during image scanning processes. Two pieces of 1.0 mm thick copper filters were attached to the machine during image acquisition to simulate soft tissue attenuation follow the method used by Jacobs et al. (46).



Figure 2 Two pieces of 1.0 mm thick copper filters were attached to the CBCT machine (Veraviewepocs 3D R100 and 3D Accuitomo 170)

Image scanning

CBCT images of each sample were acquired individually on a Veraviewepocs 3D R100 (Morita Mfg Corp, Kyoto, Japan) and 3D Accuitomo 170 (Morita Mfg Corp, Kyoto, Japan), which was operated at 90 kVp and 5 mA. Eight rounds of image scanning were performed for each tooth on each machine, before and after VRF fabrication (no-VRF and VRF groups), with and without gutta percha cone (filling and no-filling groups) and by using two FOV scans (4x4 and 8x8 cm). All 8x8 cm FOV dataset were undergone second reconstruction process to resize the image volume down to only one sample without any change in voxel size. Manufacturer resolution setting for Veraviewepocs 3D R100 for both FOV were equal at 0.125 mm, while those for 3D Accuitomo 170 were 0.08 and 0.16 mm for small and medium FOV, respectively. In conclusion, 16 CBCT images were obtained from each tooth and 640 CBCT images were received in total.

VRF Fabrication



Figure 3 Sample fixed in 2 x 2.5 cm (diameter x height) PVC tube with resin acrylic

Each sample was temporarily fixed in PVC tube (2.5 cm height and 2 cm diameters) with resin acrylic. A universal testing machine (Hounsfield H10KM, test equipment Ltd, Redhill, United Kingdom) was selected for creation of VRF for each sample by insertion of a conical metal tip in the prepared root canal. A 10,000N load cell was applied with a compression speed of 10 mm/min, which was stopped once the applied forced has dropped to prevent the displacement of the root fragment. 10% of samples were randomly selected for fracture line evaluation with micro CT (μ CT 35, SCANCO Medical, Switzerland). Then all samples were inspected by direct visual combining with transillumination to confirm the presence of VRF after VRF induction process.

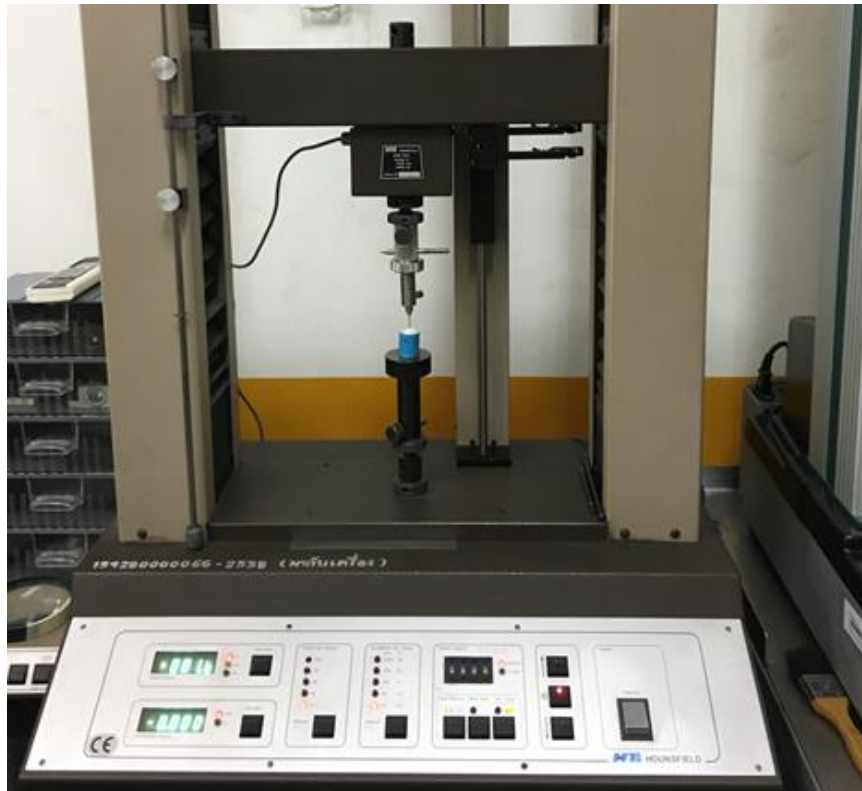


Figure 4 VRF creation by using a universal testing machine (hounsfield H10KM, test equipment Ltd, Redhill, United Kingdom)

Image analysis

Image analysis was performed by using i-Dixel software provided by each CBCT machine. An oral and maxillofacial radiologist with more than 10 years of experiences and two master degree students in Oral and Maxillofacial Radiology Department investigated for the VRF in each sample. For this, all three observers were calibrated to get more than 80 percent accuracy in VRF detection with reference data set. All images will be displayed in a low light environment with flat screen monitors using 1920 x 1080-pixel resolution. The observers analyzed the image in the axial, coronal and sagittal

reconstructions with the possibility of adjusting brightness and contrast, zooming and rotating. Example images are shown in Figure 4.

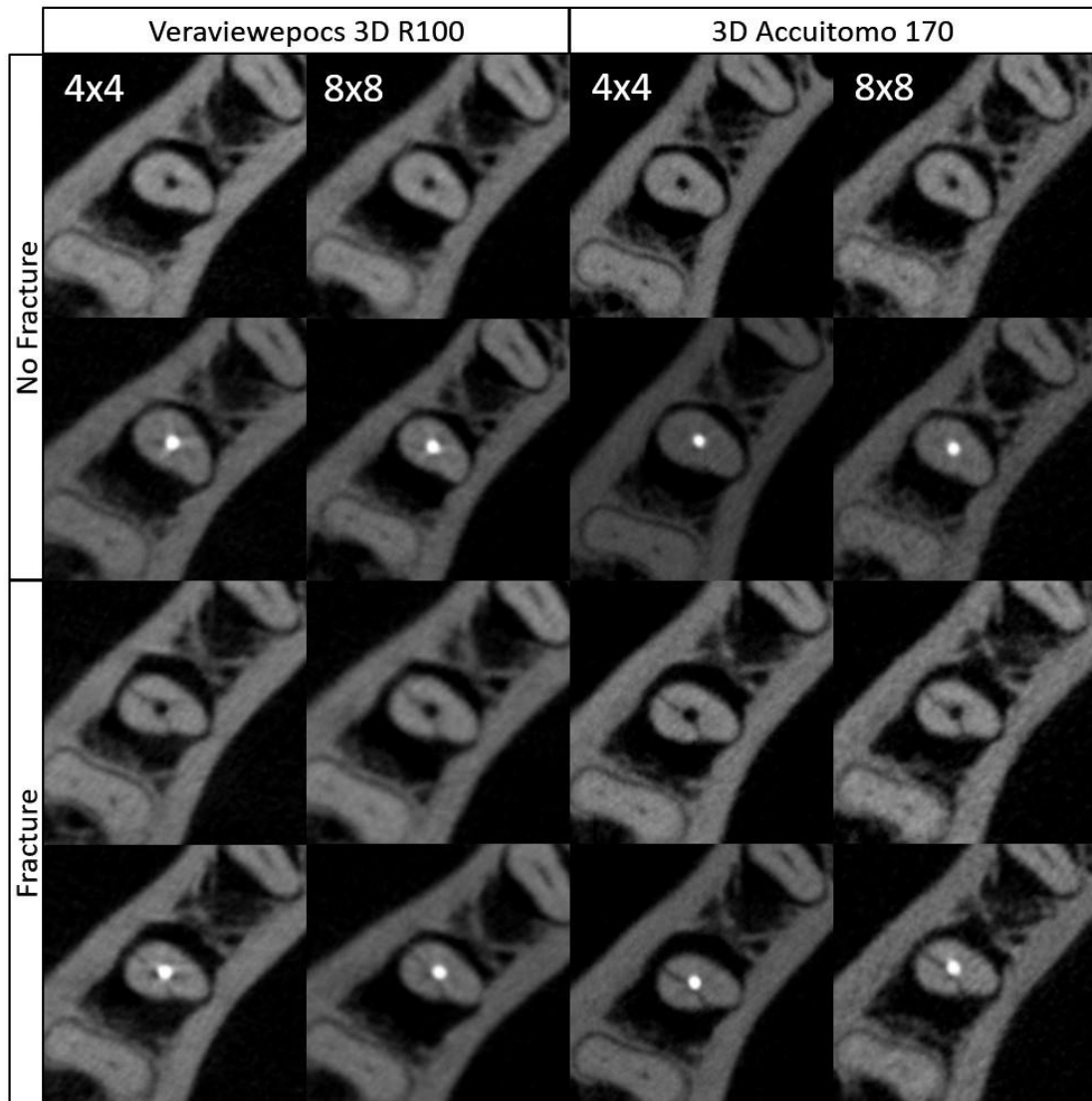


Figure 5 An example of an axial cross-section showing a vertical root fracture of hybrid CBCT (Veraviewepocs 3D R100) and CBCT (3D Accuitomo 170) using 4x4 and 8x8 cm FOV

The 5-point scoring system will be used to assess the VRF in each sample as followed:

- 1: Fracture definitely not present
- 2: Fracture probably not present
- 3: Uncertain
- 4: Fracture probably present
- 5: Fracture definitely present

If score 4 or 5 was recorded, the location of fracture line was also assessed as B (buccal), M (mesial), D (distal) and L (lingual).

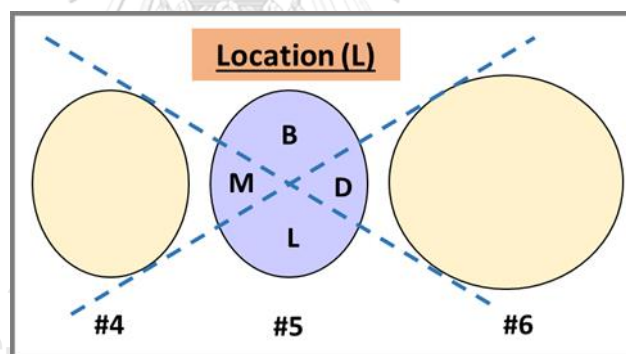


Figure 6 Location of fracture line recorded for score 4 and 5

10% of samples from each group were randomly selected and repeated the image analysis after 2 weeks by the same observers to assess intra-observer reliability.

Statistical analysis

The data was analyzed using SPSS software (Version 22.0; IBM, Armonk, NY). For dichotomized data: grouping scores 1, 2, 3 as a negative finding (absence of fracture) and scores 4 and 5 as a positive finding (presence of fracture). Cohen's kappa coefficient (k) was calculated for degree of agreement in detecting VRF (intra-observer agreement). The k -values were interpreted as slight agreement (0.01 to 0.20), fair agreement (0.21 to 0.40), moderate agreement (0.41 to 0.60), substantial agreement (0.61 to 0.80) and almost perfect agreement (0.81 to 0.99). The receiver operating characteristic (ROC) curve was used to assess the relationship between the sensitivity and specificity of both CBCT machine in the diagnosis of the VRF, and area under curved (AUC) was calculated. Before calculation, all cases with score 4 and 5 were rechecked for fracture location. Any case with incorrect location of the VRF was referred as incorrect detection of the VRF and converted from score 5 to score 1 and score 4 to score 2.

CHAPTER IV: RESULT & DISCUSSION

Result

Fracture analysis

100% agreement in VRF detection of both area and location of fracture line between using micro CT and direct visualization combining with transillumination were received. The fracture widths were range from 0.024 - 0.106 mm.

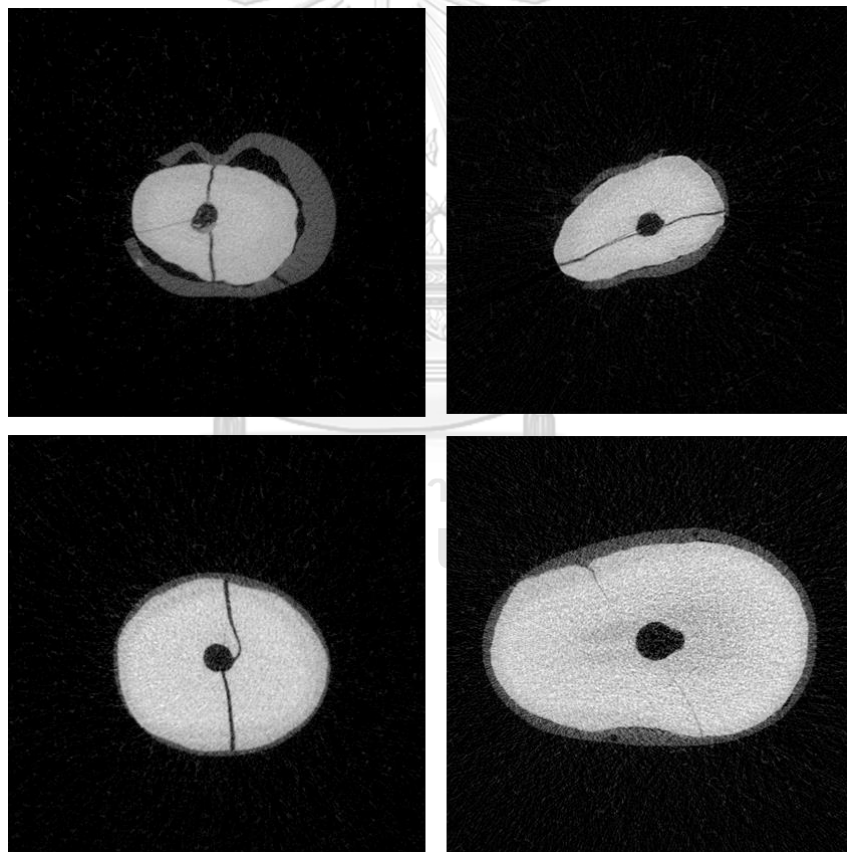


Figure 7 The micro CT images of 10% randomly selected teeth with VRF

The two and three area fracture teeth were mostly found in this study (15 teeth, 37.5%) and (14 teeth, 35.0%) followed by one area fracture teeth (9 teeth, 22.5%). Four area fracture teeth were only found in 2 teeth (5.0%). Of all fracture occurred in more than one area, most fracture line were detected in bucco-lingual direction (17 teeth, 42.5%) and mesio-distal direction (11 teeth, 27.5%). Fracture line occurred in other direction including one area fracture were observed in 12 teeth (30.0%).

Interobserver agreement and intraobserver agreement

Table 1 Interobserver agreement in the detection of vertical root fracture

	Observer 1	Observer 2	Observer 3
Observer 1		0.709	0.629
Observer 2			0.591
Observer 3			

The interobserver agreements were range from moderate agreement to substantial agreement as showed in table 1. As for intraobserver agreements, the reproducibilities were range from substantial agreement to almost perfect agreement ($k = 0.745-0.835$)

Detection of the vertical root fracture

Table 2 Diagnostic performance of each CBCT modalities

	AUC		Sensitivity		Specificity	
	Means	p-Value	Means	p-Value	Means	p-Value
Accuitomo 3D 170	0.731	>0.05	0.456	>0.05	0.958	>0.05
Veraviewepocs 3D R100	0.701		0.422		0.961	

Sensitivity, specificity and Area Under Curve (AUC) of the Veraviewepocs 3D R100 CBCT and 3D Accuitomo 170 CBCT in detection of the VRF were listed in Table 2. Paired T-test was used to compare means between each modality. 3D Accuitomo 170 showed slightly higher in both AUC and sensitivity, but no significant differences were detected.

Table 3 Diagnostic performance of each scanning protocols

		AUC		Sensitivity		Specificity	
		Means	p-Value	Means	p-Value	Means	p-Value
FOV	4 x 4	0.716	>0.05	0.453	>0.05	0.950	>0.05
	8 x 8	0.717		0.422		0.972	
Gutta percha	Without	0.748	>0.05	0.478	>0.05	0.978	>0.05
	With	0.691		0.407		0.945	

Sensitivity, specificity and area under curve (AUC) in detection of the VRF using various scanning protocols were recorded in table 3.

Table 4 Area under ROC curved showing diagnostic performance of hybrid CBCT and CBCT using 2 different FOVs

	FOV 4x4		FOV 8x8	
	AUC	p-Value	AUC	p-Value
3D Accuitomo 170	0.736	>0.05	0.723	>0.05
Veraviewepocs 3D R100	0.695		0.710	

Table 5 Sensitivity and specificity in VRF detection with 4x4 and 8x8 cm FOV from hybrid CBCT and CBCT using 2 difference FOVs

	FOV 4x4				FOV 8x8			
	Sensitivity	p-Value	Specificity	p-Value	Sensitivity	p-Value	Specificity	p-Value
3D Accuitomo 170	0.475	>0.05	0.950	>0.05	0.431	>0.05	0.969	>0.05
Veraviewepocs 3D R100	0.430		0.950		0.412		0.975	

Table 6 Area under ROC curved showing diagnostic performance of hybrid CBCT and CBCT with and without Gutta percha cone

	Without gutta percha		With gutta percha	
	AUC	p-Value	AUC	p-Value
3D Accuitomo 170	0.750	>0.05	0.716	>0.05
Veraviewepocs 3D R100	0.746		0.667	

Table 7 Sensitivity and specificity in VRF detection with 4x4 and 8x8 cm FOV from hybrid CBCT and CBCT with and without Gutta percha cone

	<u>Without gutta percha</u>				<u>With gutta percha</u>			
	Sensitivity	p-Value	Specificity	p-Value	Sensitivity	p-Value	Specificity	p-Value
3D Accuitomo 170	0.475	>0.05	0.981	>0.05	0.440	>0.05	0.940	>0.05
Veraviewepocs 3D R100	0.481		0.975		0.375		0.950	

Sensitivity, specificity and area under curve (AUC) of the Veraviewepocs 3D R100 CBCT and 3D Accuitomo 170 CBCT in detection of the VRF using various scanning protocols were reviewed in table 4-7.

Images scanning with FOV of 4x4 also had higher performance in detection of the VRF compared to those scanning with FOV of 8x8. Moreover, Presentation of gutta percha also have an effect in the VRF detection, which result in reduction of accuracy in diagnostic of the VRF in overall modalities. Still, no significance differences were found.

Discussion

This study investigated the accuracy in detection of the VRF by using CBCT and also compared two CBCT systems including hybrid CBCT and conventional CCBCT with various type of scanning protocols. The results of this study showed that 3D Accuitomo 170, which represent conventional CBCT system, has slightly higher accuracy in identifying VRF in overall protocols compared to Veraviewepocs 3D R100, which represent hybrid CBCT system.

Accuracy of each CBCT systems based on various factors such as exposure setting, detector type, FOV selection and voxel size as well as system specific image artifacts (32). Because both 3D Accuitomo 170 and Veraviewepocs 3D R100 using same exposure setting and flat-panel detectors (FPDs), thus exposure settings and detector type had no effect in this study. Still, Katsumata et al. (48) reported that FPDs were superior to image intensifier tube/charged coupled device (IIT/CCD) with lower image distortion, better spatial resolution, higher dynamic range and reduction of noise and image artifacts. Kajan and Taromsari (2012) also reported that CBCT using FPDs is superior to other types in detecting the VRF.

The number of basis images are directly related to the amount of information generated for image reconstruction. A greater number of basis images provide more information in image reconstruction resulted in a smoother images and reduction of image noise and image artifacts (39). This could be another reason that 3D Accuitomo

170 with 360° of rotation and 577 basis images per scan, had better accuracy compared to Veraviewepocs 3D R100 with 180 ° of rotation and 367 basis images per scan. Nevertheless, a larger number of basis images will increase the scanning time, the longer reconstruction time, the higher radiation dose to the patient (49).

Concern over radiation exposure is also a factor in choosing among imaging modalities. A recent study of CBCT found that smaller FOV result in lower effective doses. Thus choosing a proper FOV for each case is also importance (4) .

In this current study, 3D Accuitomo 170 has higher computed tomography dose index (CTDIvol), at 90 kVp and 5 mA, compared to Veraviewepocs 3D R100 as shown in table 8. Also, with larger FOV, more radiation dose was detected.

Table 8 CTDIvol of each CBCT in difference FOVs as shown in operation guideline

Modality		CTDIvol
3D Accuitomo 170	4 x 4	4.60
	8 x 8	6.60
Veraviewepocs 3D R100	4 x 4	4.06
	8 x 8	5.52

FOV selection were directly related to voxel size, which is the smallest element of the 3D radiograph image volume (11). The smaller of the voxel size, the better of the quality of the picture due to more capability in visualization of a very small changes of the structure (10). Partial volume averaging is another type of CBCT artifact that may affect the visibility of VRF. These occurred when the selected voxel size is greater than the spatial or contrast resolution of the object to be imaged. Resulting in weighted average of the difference CT value at the border of the object which will appear as a homogeneity of pixel intensity levels of the image boundaries (39). Thus, for a very small fracture line, too large voxel size can cause disappearance of the VRF in CBCT. To reduce this artifact, choosing a smaller voxel can be useful. Therefore, for higher accuracy in diagnostic of the VRF, a smaller FOV and smaller corresponding voxel size were recommended (2). In the present study, using FOV of 4x4 also showed slightly higher accuracy in detecting the VRF compared to using FOV of 8x8 for both CBCT systems. 3D Accuitomo 170 still had slightly better accuracy compared to Veraviewepocs 3D R100, But with no significant association. The explanation of this result may be due to difference in voxel size for each FOV selection of each CBCT machine. Veraviewepocs 3D R100 had the same voxel size of 0.125 mm for both 4x4 and 8x8 FOV, whereas 3D Accuitomo 170 had voxel size of 0.08 mm and 0.16 mm for FOV of 4x4 and 8x8 respectively. As above, 3D Accuitomo 170 had smaller voxel size for 4x4 FOV but larger voxel size in 8x8 FOV. A recent study also suggest that the

greater probability of correctly identifying root fractures occurred when the image was acquired by using the smaller voxel resolution parameter (28). However, Ozer (34) reported that voxel size of 0.125 mm and 0.2 mm had no significant differences in terms of sensitivity and specificity. A study from Huang et al.(50) concluded that CBCT with voxel size greater than 0.2mm may not be suitable for clinical identification of most VRFs. Selection of FOV with 0.08 mm voxel size were more favorable in VRF detection.

Although CBCT had been chosen to be the imaging modality of choice for the diagnosis and management of the root fractures by AAE, production of beam hardening artifact still be one of a major disadvantage of CBCT (5). These artifacts produced by high density object which will absorb more low-energy photons than high-energy photons which result in higher mean energy passed through (14). The presence of radiopaque intracanal materials will act as artifact creating factor and resulted in beam hardening phenomenon which created the radiolucent and radiopaque lines around the materials (51). These imaging artefacts could present similarly to root fractures and thus lead to false positive readings and resulted in the overestimation of VRF detection with and also the overall inaccuracy of this system (4, 52). In this study, the result also showed that there was slightly higher accuracy in detection of the VRF when no gutta percha presented in root canal. Moreover, 3D Accuitomo 170 still had slightly better accuracy for both present and absence of intracanal material, but no significant difference was recorded. A study from Wang et al. (53) reported that the sensitivity of

CBCT in the detection of VRF was reduced in root with presented of intracanal material compared with absence ones. And also reported that 'star-shaped streak artefacts', may compromised the quality of the images, thus 'decreasing the observers' confidence' therefore resulting in a reduced sensitivity. Hassan et al. (54) described that CBCT specificity was reduced in the presence of root canal fillings, however its overall accuracy was not influenced. Another research from Melo et al. (28) was to evaluate the influence of intra canal material such as, cast-gold posts and gutta percha cone on the VRF detection ability of CBCT. They conclude that presentation of intracanal material could reduce the overall CBCT diagnostic ability of the VRF, but with no significant difference detected, which is similar to this study. Another explanation could be that slightly upward of rotation angle produced by Veraviewepocs 3D R100 which may create more artifacts than horizontal rotation angle produced 3D Accuitomo 170. These upward angulations can normally find in most hybrid CBCT system. Due to combination of a digital panoramic, same x-ray source must be use for both 3D system and 2D system. However, to our knowledge, there are still no study support the effect of upward angulation on artifact creation.

According to the literature reviewed, many imitations with an in vitro model study were recorded. First, the results from the present study are not directly applicable to a clinical situation. In clinical situations, assessment of the VRF not only can be diagnosed by the presence of the fracture itself but also the shape, localization, and size of bone

resorption adjacent to the fracture line. Thus, in vivo, the fracture line may not be detected, but can be diagnosed by other condition of surrounding structures (55). Moreover, the presence of a tooth crown and/or prosthetic materials could affect the observation of VRF in the cervical axial slices adjacent to the cementoenamel junction which were exclude in this present study (28).

Conclusion

This study demonstrated that the abilities of CBCT and hybrid CBCT in detecting VRF are similarly, still, CBCT show a slightly higher performance. FOV and voxel size selection also influence the VRF investigation. With smaller FOV and voxel size, better VRF detection is achieved. Furthermore, presentation of root canal filling material reduces diagnostic ability of the VRF for overall CBCT systems. However, further researches are required.

REFERENCES

1. Garcia-Guerrero C, Parra-Junco C, Quijano-Guauque S, Molano N, Pineda GA, Marin-Zuluaga DJ. Vertical root fractures in endodontically-treated teeth: A retrospective analysis of possible risk factors. *Journal of Investigative and Clinical Dentistry*. 2018;9(1).
2. Huang C-C, Lee B-S. Diagnosis of vertical root fracture in endodontically treated teeth using computed tomography. *Journal of Dental Sciences*. 2015;10(3):227-32.
3. Khasnis SA, Kidiyoor KH, Patil AB, Kenganal SB. Vertical root fractures and their management. *Journal of conservative dentistry*. 2014;17(2):103-10.
4. Kamburoglu K, Murat S, Yüksel SP, Cebeci ARI, Horasan S. Detection of vertical root fracture using cone-beam computerized tomography: an in vitro assessment. *Oral Surgery, Oral Medicine, Oral Pathology, Oral Radiology, and Endodontology*. 2010;109(2):74-81.
5. Neves FS, Freitas DQ, Campos PSF, Ekestubbe A, Lofthag-Hansen S. Evaluation of cone-beam computed tomography in the diagnosis of vertical root fractures: the influence of imaging modes and root canal materials. *Journal of endodontics*. 2014;40(10):1530-6.
6. Willy SRK, Dorothea B, Bernd DH. On cone-beam computed tomography artifacts induced by titanium implants. *Clinical Oral Implants Research*. 2010;21(1):100-7.
7. Dutra KL, Pachêco-Pereira C, Bortoluzzi EA, Flores-Mir C, Lagravère MO, Corrêa M. Influence of intracanal materials in vertical root fracture pathway detection with cone-

beam computed tomography. *Journal of endodontics*. 2017;43(7):1170-5.

8. Abramovitch K, Rice DD. Basic principles of cone beam computed tomography. *Dental Clinics of North America*. 2014;58(3):463-84.

9. Scarfe WC, Li Z, Aboelmaaty W, Scott S, Farman AG. Maxillofacial cone beam computed tomography: essence, elements and steps to interpretation. *Australian dental journal*. 2012;57(1):46-60.

10. Flint DJ, Casian Ruiz Velasco R. Cone-beam computed tomography (CBCT) applications in dentistry. Online Course: www.dentalcare.com/en-us/professional-education/ce-courses/ce531. 2017.

11. Farman AG. Evolution of CBCT: the tree now has two distinct branches. *Oral Surgery, Oral Medicine, Oral Pathology, Oral Radiology and Endodontics*. 2009;107(4):449.

12. Dillenseger JP, Gros CI, Sayeh A, Rasamimanana J, Lawniczak F, Leminor JM, et al. Image quality evaluation of small FOV and large FOV CBCT devices for oral and maxillofacial radiology. *Dentomaxillofacial Radiology*. 2016;46(1).

13. Kiljunen T, Kaasalainen T, Suomalainen A, Korttinen M. Dental cone beam CT: a review. *European Journal of Medical Physics*. 2015;31(8):844-60.

14. Esmaeili F, Johari M, Haddadi P, Vatankhah M. Beam hardening artifacts: comparison between two cone beam computed tomography scanners. *Journal of Dental*

Research, Dental Clinics, Dental Prospects. 2012;6(2):49-53.

15. Rivera E, Walton RE. Cracking the Cracked Tooth Code. ENDODONTICS: COLLEAGUES FOR EXCELLENCE NEWSLETTER. SUMMER 2008.

16. Alsani A, Balhaddad A, Nazir MA. Vertical root fracture: a case report and review of the literature. Giornale italiano di endodonzia. 2017;31(1):21-8.

17. Tamse A. Vertical root fractures in endodontically treated teeth: diagnostic signs and clinical management. Endodontic topics. 2006;13(1):84-94.

18. Liao W-C, Tsai Y-L, Wang C-Y, Chang M-C, Huang W-L, Lin H-J, et al. Clinical and radiographic characteristics of vertical root fractures in endodontically and nonendodontically treated teeth. Journal of endodontics. 2017;43(5):687-93.

19. Yoshino K, Ito K, Kuroda M, Sugihara N. Prevalence of vertical root fracture as the reason for tooth extraction in dental clinics. Clinical oral investigations. 2015;19(6):1405-9.

20. Özer SY, Ünlü G, Değer Y. Diagnosis and treatment of endodontically treated teeth with vertical root fracture: three case reports with two-year follow-up. Journal of endodontics. 2011;37(1):97-102.

21. Brady E, Mannocci F, Brown J, Wilson R, Patel S. A comparison of cone beam computed tomography and periapical radiography for the detection of vertical root fractures in nonendodontically treated teeth. International Endodontic Journal. 2014;47(8):735-46.

22. Fuss Z, Lustig J, Katz A, Tamse A. An evaluation of endodontically treated vertical root fractured teeth: impact of operative procedures. *Journal of Endodontics*. 2001;27(1):46-8.
23. Cohen S, Blanco L, Berman L. Vertical root fractures: Clinical and radiographic diagnosis. *The Journal of the American Dental Association*. 2003;134(4):434-41.
24. Moule AJ, Kahler B. Diagnosis and management of teeth with vertical root fractures. *Australian dental journal*. 1999;44(2):75-87.
25. Wang P, Su L. Clinical observation in 2 representative cases of vertical root fracture in nonendodontically treated teeth. *Oral Surgery, Oral Medicine, Oral Pathology, Oral Radiology, and Endodontology*. 2009;107(4):e39-e42.
26. Ferreira LM, Visconti MAPG, Nascimento HA, Dallemolle RR, Ambrosano GM, Freitas DQ. Influence of CBCT enhancement filters on diagnosis of vertical root fractures: a simulation study in endodontically treated teeth with and without intracanal posts. *Dentomaxillofacial Radiology*. 2015;44(5):20140352.
27. Corbella S, Tamse A, Nemcovsky C, Taschieri S. Diagnostic issues dealing with the management of teeth with vertical root fractures: a narrative review. *Giornale Italiano di Endodonzia*. 2014;28(2):91-6.
28. Melo SLS, Bortoluzzi EA, Abreu M, Corrêa LR, Corrêa M. Diagnostic Ability of a Cone-Beam Computed Tomography Scan to Assess Longitudinal Root Fractures in

Prosthetically Treated Teeth. *Journal of Endodontics*. 2010;36(11):1879-82.

29. Byakova SF, Novozhilova NE, Makeeva IM, Grachev VI, Kasatkina IV. The accuracy of CBCT for the detection and diagnosis of vertical root fractures in vivo. *International Endodontic Journal*. 2019;52(9):1255-63.

30. Rivera EM, Walton RE. Longitudinal tooth fractures: findings that contribute to complex endodontic diagnoses. *Endodontic Topics*. 2007;16(1):82-111.

31. Ghorbanzadeh A, Aminifar S, Shadan L, Ghanati H. Evaluation of three methods in the diagnosis of dentin cracks caused by apical resection. *Journal of Dentistry (Tehran, Iran)*. 2013;10(2):175.

32. Hassan B, Metska ME, Ozok AR, van der Stelt P, Wesselink PR. Comparison of five cone beam computed tomography systems for the detection of vertical root fractures. *Journal of endodontics*. 2010;36(1):126-9.

33. Kataoka ML, Hochman MG, Rodriguez EK, Lin P-JP, Kubo S, Raptopoulos VD. A review of factors that affect artifact from metallic hardware on multi-row detector computed tomography. *Current Problems in Diagnostic Radiology*. 2010;39(4):125-36.

34. Ozer SY. Detection of vertical root fractures by using cone beam computed tomography with variable voxel sizes in an in vitro model. *Journal of endodontics*. 2011;37(1):75-9.

35. Durack C, Patel S, Davies J, Wilson R, Mannocci F. Diagnostic accuracy of small

volume cone beam computed tomography and intraoral periapical radiography for the detection of simulated external inflammatory root resorption. *International Endodontic Journal*. 2011;44(2):136-47.

36. Liedke Gabriela S, Spin-Neto R, Silveira Heloisa ED, Schropp L, Stavropoulos A, Wenzel A. Factors affecting the possibility to detect buccal bone condition around dental implants using cone beam computed tomography. *Clinical Oral Implants Research*. 2017;28(9):1082-8.

37. Chindasombatjaroen J, Kakimoto N, Murakami S, Maeda Y, Furukawa S. Quantitative analysis of metallic artifacts caused by dental metals: comparison of cone-beam and multi-detector row CT scanners. *Oral Radiology*. 2011;27(2):114-20.

38. Jaju PP, Jain M, Singh A, Gupta A. Artefacts in cone beam CT. *Open Journal of Stomatology*. 2013;3(5):6.

39. Scarfe WC, Farman AG. What is Cone-Beam CT and How Does it Work? *Dental Clinics*. 2008;52(4):707-30.

40. Vasconcelos KF, Nicolielo LFP, Nascimento MC, Haiter-Neto F, Bóscolo FN, Van Dessel J, et al. Artefact expression associated with several cone-beam computed tomographic machines when imaging root filled teeth. *International Endodontic Journal*. 2015;48(10):994-1000.

41. Rabelo KA, Cavalcanti YW, de Oliveira Pinto MG, Sousa Melo SL, Campos PSF, de

Andrade Freitas Oliveira LS, et al. Quantitative assessment of image artifacts from root filling materials on CBCT scans made using several exposure parameters. *Imaging science in dentistry*. 2017;47(3):189-97.

42. Pauwels R, Araki K, Siewerdsen JH, Thongvigitmanee SS. Technical aspects of dental CBCT: state of the art. *Dentomaxillofacial Radiology*. 2015;44(1):20140224.

43. Miracle AC, Mukherji SK. Conebeam CT of the head and neck, part 1: physical principles. *American Journal of Neuroradiology*. 2009;30:1088-95.

44. Schulze R, Heil U, Grob D, Bruellmann D, Dranischnikow E, Schwanecke U, et al. Artefacts in CBCT: a review. *Dentomaxillofacial Radiology*. 2011;40(5):265-73.

45. Wanderley VA, Freitas DQ, Haiter-Neto F, Oliveira ML. Influence of Tooth Orientation on the Detection of Vertical Root Fracture in Cone-beam Computed Tomography. *Journal of endodontics*. 2018.

46. Jacobs R, Pittayapat P, Bornstein MM, Imada TSN, Coucke W, Lambrichts I. Accuracy of linear measurements using three imaging modalities: two lateral cephalograms and one 3D model from CBCT data. *European Journal of Orthodontics*. 2014;37(2):202-8.

47. Elsaltani MH, Farid MM, Ashmawy MSE. Detection of simulated vertical root fractures: which cone-beam computed tomographic system is the most accurate? *Journal of endodontics*. 2016;42(6):972-7.

48. Katsumata A, Hirukawa A, Okumura S, Naitoh M, Fujishita M, Aiji E, et al. Effects of image artifacts on gray-value density in limited-volume cone-beam computerized tomography. *Oral Surgery, Oral Medicine, Oral Pathology, Oral Radiology, and Endodontology*. 2007;104(6):829-36.
49. Wanderley VA, Neves FS, Nascimento MCC, Monteiro GQM, Lobo NS, Oliveira ML, et al. Detection of Incomplete Root Fractures in Endodontically Treated Teeth Using Different High-resolution Cone-beam Computed Tomographic Imaging Protocols. *Journal of endodontics*. 2017;43(10):1720-4.
50. Huang C-C, Chang Y-C, Chuang M-C, Lin H-J, Tsai Y-L, Chang S-H, et al. Analysis of the Width of Vertical Root Fracture in Endodontically Treated Teeth by 2 Micro-Computed Tomography Systems. *Journal of Endodontics*. 2014;40(5):698-702.
51. Hekmatian E, Karbasi Kheir M, Fathollahzade H, Sheikhi M. Detection of Vertical Root Fractures Using Cone-Beam Computed Tomography in the Presence and Absence of Gutta-Percha. *The Scientific World Journal*. 2018;2018:1-5.
52. Patel S, Brady E, Wilson R, Brown J, Mannocci F. The detection of vertical root fractures in root filled teeth with periapical radiographs and CBCT scans. *International Endodontic Journal*. 2013;46(12):1140-52.
53. Wang P, Yan X, Lui D, Zhang W, Zhang Y, Ma X. Detection of dental root fractures by using cone-beam computed tomography. *Dentomaxillofacial Radiology*.

2011;40(5):290-8.

54. Hassan B, Metska ME, Ozok AR, van der Stelt P, Wesselink PR. Detection of vertical root fractures in endodontically treated teeth by a cone beam computed tomography scan. *Journal of endodontics*. 2009;35(5):719-22.

55. Fayad MI, Ashkenaz PJ, Johnson BR. Different Representations of Vertical Root Fractures Detected by Cone-Beam Volumetric Tomography: A Case Series Report. *Journal of Endodontics*. 2012;38(10):1435-42.





จุฬาลงกรณ์มหาวิทยาลัย
CHULALONGKORN UNIVERSITY

VITA

NAME Nantida Ruengweerayut
DATE OF BIRTH 5 October 1990
PLACE OF BIRTH Nonthaburi
INSTITUTIONS ATTENDED Faculty of dental medicine, Rangsit university
HOME ADDRESS 216 Anan dental clinic, Tiwanond Rd, Mueng, Nonthaburi,
11000

